Division of labor in metabolic regulation by transcription, translation, acetylation and phosphorylation

Sriram Chandrasekaran[1,2,*]

[1] - Department of Biomedical Engineering, [2] - Center for Computational Medicine and Bioinformatics, University of Michigan, Ann Arbor, MI, USA, 48109

* - Correspondence: csriram@umich.edu

Abstract

The metabolism of most organisms is controlled by a diverse cast of regulatory processes, including transcriptional regulation and post-translational modifications (PTMs). Yet how metabolic control is distributed between these regulatory processes is unknown. Here we present *Comparative Analysis of Regulators of Metabolism* (CAROM), an approach that compares regulators based on network connectivity, flux, and essentiality of their reaction targets. Using CAROM, we analyze transcriptome, proteome, acetylome and phospho-proteome dynamics during transition to stationary phase in *E. coli* and *S. cerevisiae*. CAROM uncovered that the targets of each regulatory process shared unique metabolic properties: growth-limiting reactions were regulated by acetylation, while isozymes and futile-cycles were preferentially regulated by phosphorylation. Reversibility, essentiality, and molecular-weight further distinguished reactions controlled through diverse mechanisms. While every enzyme can be potentially regulated by multiple mechanisms, analysis of context-specific datasets reveals a conserved partitioning of metabolic regulation based on reaction attributes.

Author summary

There are several ways to regulate an enzyme's activity in a cell. Yet, the design principles that determine when an enzyme is regulated by transcription, translation or post-translational modifications are unknown. Each control mechanism, such as transcription, comprises several regulators that control a distinct set of targets. So far, it is unclear if similar partitioning of targets occurs at a higher level, between different control mechanisms. Here we systematically analyze patterns of metabolic regulation in model microbes. We find that five key parameters can distinguish the targets of each mechanism. These key parameters provide insights on specific roles played by each mechanism in determining overall metabolic activity. This approach may help define the basic regulatory architecture of metabolic networks.

Introduction

A myriad control mechanisms regulate microbial metabolic adaptation to new environments [1–8]. Nevertheless, microbes deploy distinct regulatory mechanisms to regulate enzyme activity in response to specific environmental challenges. For example, *B. subtilis* cells primarily utilize transcriptional regulation when glucose is available, but post-transcriptionally regulate metabolic enzymes after malate addition [9]. In both *E. coli* and yeast, some pathways, such as glycolysis, are predominantly regulated by post-transcriptional regulation, while others, such as the TCA cycle, are regulated at the transcriptional level [1,3,10]. This suggest that apart from differences in response time, specific mechanisms are deployed for specialized regulatory tasks. Nevertheless, it is unclear why some enzymes are regulated using acetylation or via other PTMs such as phosphorylation [3,4].

Numerous advantages of regulation by PTMs have been proposed over the past five decades [11–13]. These include low energy requirements, rapid response, and signal amplification. Yet these

1

42 characteristics are not unique to PTMs, and these features also do not differentiate between PTMs
43 such as acetylation and phosphorylation. The staggering complexity of each regulatory process has
44 limited the comparative analysis of metabolic regulation at a systems level [3]. Existing studies have
45 focused on a small set of metabolic pathways or on a single regulatory process [4,10,14–20]. Such
46 studies have revealed reaction reversibility and metabolic network structure to be predictive of
47 regulation [8,16,21–24]. Yet these studies do not shed light on the differences between each regulatory
48 process. In sum, although some general network principles of regulation are known, how it is
49 partitioned among various regulatory mechanisms is unclear.

50 We hence developed a data-driven approach, called *Comparative Analysis of Regulators of Metabolism*
51 (CAROM), to identify unique features of each regulatory process. CAROM achieves this by comparing
52 various properties of metabolic enzymes, including essentiality, flux, molecular weight and topology. It
53 identifies those properties that are highly enriched among targets of each process than expected out of
54 random chance.

Results and Discussion

56 Here we focus on four well-studied control mechanisms with available omics datasets - transcription,
57 post-transcription, phosphorylation and acetylation. We analyzed the dynamics of metabolic regulation
58 during a well-characterized process in yeast, namely, transition to stationary phase. We obtained RNA
59 sequencing, time-course proteomics, acetylomics, and phospho-proteomics data from the literature
60 [25–27]. Targets for each process were determined based on differential levels between stationary and
61 exponential phase (Methods). We assumed that PTMs and other regulatory sites that are dynamic and
62 conditionally regulated are likely to be functional [28].

63 The targets of diverse regulatory mechanisms were used as input to CAROM. CAROM analyzes the
64 properties of the targets in the context of a genome-scale metabolic network model of yeast [29]. We
65 hypothesized that differences in target preferences between diverse regulators can be inferred from the
66 network topology and fluxes. Protein and gene targets of each process were mapped to corresponding
67 metabolic reactions in the model. There was significant overlap among reactions regulated through
68 changes in both the transcriptome and proteome, and transcriptome and acetylome (hypergeometric p-
69 value = 5×10^{-25} and 1×10^{-15} respectively; S. Table 1). In contrast, there was little overlap between
70 targets of phosphorylation with other mechanisms (p-value > 0.1; S. Table 1). While prior studies found
71 higher overlap between targets of PTMs [30,31], they used all possible sites that can be acetylated or
72 phosphorylated. However, only a fraction of PTM sites are likely to be active and functional in a single
73 condition. Overall, each regulatory mechanism had a distinct set of targets (Figure 1A).

74 What are the common features of enzymes that are regulated by each mechanism? To answer this, we
75 used CAROM to compare the regulation of enzymes that are essential for growth in minimal media.
76 Essential enzymes in the yeast metabolic model were determined using Flux Balance Analysis (FBA)
77 [32]. Surprisingly, this set of enzymes was highly enriched among those regulated by acetylation but
78 not by other processes (ANOVA p-value < 10^{-16}; Figure 1B; S. Table 2). Since regulation can be
79 optimized for fitness across multiple conditions [33], we identified enzymes that impact growth in 87
80 different nutrient conditions comprising various carbon and nitrogen sources using FBA. This set of
81 essential enzymes was once again enriched for acetylation relative to other mechanisms (ANOVA p-
82 value < 10^{-16}; S. Figure 1). This trend was observed using experimentally derived list of essential genes
83 as well (hypergeometric p-value = 2×10^{-7} for acetylation). Interestingly, in contrast to acetylation,
84 genes regulated at the proteomic level were significantly under-represented among the essential genes
85 (hypergeometric p-value of depletion = 8×10^{-11}). Thus, essential enzymes are likely to be constitutively

86 expressed and their activity modulated through acetylation. This may explain why transcriptional
87 regulation has minimal impact on fluxes in central metabolism, which contain several growth-limiting
88 enzymes [3,10].

89 We next used CAROM to determine the impact of reaction position in the network on its regulation. We
90 counted the number of pathways each reaction is involved in, along with other topological metrics, such
91 as the closeness, degree and page rank. We found that the regulation of enzymes differed significantly
92 based on network topology (Figure 1C). First, reactions with low connectivity, measured through any of
93 the topological metrics, were highly likely to be unregulated. In contrast, highly connected enzymes
94 linking multiple pathways were more likely to be regulated by PTMs. Interestingly, reactions regulated
95 by both the PTMs had the highest connectivity (S. Figures 2, 3). Several key hubs, such as acetyl-CoA
96 acetyltransferase, hexokinase and phosphofructokinase are regulated by at least 2 different
97 mechanisms (S. Table 3).

98 We next assessed how regulation differs based on the magnitude and direction of flux through the
99 network. We inferred the full range of fluxes possible through each reaction using flux variability
100 analysis (FVA) [34]. Since yeast cells may not optimize their metabolism for biomass synthesis during
101 transition to stationary phase, we also performed FVA without assuming biomass maximization. We
102 found that irreversible reactions were highly likely to be regulated (S. Figure 4). A recent study found
103 the same trend for allosteric regulation as well [21]. However, reversibility alone did not differentiate
104 between regulatory mechanisms.

105 Interestingly, reactions that have the potential to carry high fluxes were predominantly regulated by
106 phosphorylation (Figure 1D; ANOVA p-value < 10^{-16}). This set of phosphorylated reactions comprise
107 several kinase-phosphatase pairs, enzymes that are part of loops that consume energy ("futile cycles"),
108 or reactions that have isozymes in compartments such as vacuoles or nucleus (S. Table 4). Thus,
109 phosphorylation in this condition selectively regulates reactions to avoid futile cycling between
110 antagonizing reactions or those operating in different compartments. Using data from experimentally
111 constrained fluxes from Hackett *et al* study [21] revealed similar patterns of regulation (S. Figure 5).
112 Reactions with the highest flux, such as ATP synthase, phosphofructokinase, and nucleotide kinase,
113 were also regulated by multiple mechanisms.

114 Finally, we compared regulation based on fundamental enzyme properties: catalytic activity and
115 molecular weight. While catalytic activity was similar across the targets of all mechanisms, targets of
116 phosphorylation had the highest molecular weight (p-value < 10^{-16}) (S. Figures 6,7). There is a weak
117 correlation between molecular weight and maximum flux (Pearson's correlation R = 0.02), suggesting
118 that both maximum flux and molecular weight are likely to be independent predictors of regulation by
119 phosphorylation.

120 To check if this pattern of regulation is observed in other conditions, using CAROM, we analyzed data
121 from nitrogen starvation response and the cell cycle in yeast, where both phospho-proteomics and
122 transcriptomics data are available [35–38]. A similar trend of regulation was observed in these
123 conditions with phosphorylation regulating isozymes and enzymes that can carry high fluxes (futile
124 cycles) (Figure 2). Since isozymes arise frequently from gene duplication, our results may explain the
125 observation that duplicated genes are more likely to be regulated by phosphorylation [39].

126 Since many mechanisms of metabolic regulation are evolutionarily conserved, we next analyzed data
127 from *E. coli* cells during stationary phase [40–42]. By analyzing transcriptomics, proteomics,
128 acetylomics and phosphoproteomics data using the *E. coli* metabolic network model, CAROM
129 uncovered that the pattern of regulation observed in yeast was also observed in *E. coli* (Figure 3).

130   Reactions that were regulated in *E. coli* had higher topological connectivity compared to those that
131   were unregulated. Further, essential reactions were enriched for regulation by acetylation, and
132   reactions with high maximum flux or large enzyme molecular weight were enriched for regulation by
133   phosphorylation. However, in contrast to yeast, phosphorylation impacted very few metabolic genes in
134   *E. coli,* and may play a relatively minor role in this specific context. Phosphorylation had 20-fold fewer
135   targets compared to other mechanisms, and its targets overlapped significantly with other processes
136   (S. Tables 5-6).

137   In sum, our analysis reveals a unique distribution of regulation within the metabolic network (Figure 4).
138   Within each process, it is well known that individual regulators such as transcription factors or kinases
139   have their own unique set of targets. Here we find that similar specialization occurs at a higher scale,
140   involving diverse processes. Reaction properties identified by CAROM to be associated with distinct
141   regulatory mechanisms may be related to specific functions performed by each regulator. For example,
142   phosphorylation may represent a mechanism of feedback regulation to control futile cycles and high
143   flux reactions that consume ATP [6,43]. Finally, this pattern of regulation is context specific – predictive
144   features such as reaction flux or essentiality can change between conditions and influence regulation.
145   Further, while most essential reactions were regulated, a small subset (14%) were not found to be
146   regulated by any mechanism. These enzymes could be sites of allosteric regulation or other regulatory
147   mechanisms not covered here due to the lack of context specific datasets (S. Table 7). Overall, these
148   results are robust to the thresholds used for finding differentially regulated sites, using data from
149   different sources, and other modeling parameters (S. Tables 8-12).

150   Since microbes exhibit a wide range of metabolic behaviors, it is not possible to uncover regulation in
151   each condition through experiments. We need tools like CAROM to identify factors that determine the
152   deployment of regulatory mechanisms in a metabolic context. Although flux balance analysis of
153   metabolic models can accurately forecast optimal flux distribution, it does not provide insights on how
154   the flux rewiring is achieved. Our analysis predicts regulatory mechanisms that will likely orchestrate
155   flux adjustments based on reaction attributes. This can guide drug discovery and metabolic engineering
156   efforts by identifying regulators that are dominant in different parts of the network [44]. CAROM can be
157   applied to uncover target specificities of other regulators such as non-coding RNAs and PTMs, and
158   help understand the architecture of metabolic regulation in a wide range of organisms.

159

160

161

162

163

164

165

166

167

Methods

CAROM

The CAROM approach takes as input a list of genes that are the targets of one or more regulatory processes. It compares the properties of the targets and identifies significant differences in target properties between mechanisms using ANOVA. Overall, CAROM compares the following 13 properties:

- Impact of gene knockout on biomass production, ATP synthesis, and viability across 87 different conditions
- Flux through the network measured through Flux Variability analysis and PFBA, reaction reversibility
- Enzyme molecular weight and catalytic activity
- The total pathways each reaction is involved in, its Degree, Closeness and PageRank

The CAROM source-code is available from the Synapse bioinformatics repository https://www.synapse.org/CAROM

Processing omics data

We used RNA-sequencing data from Treu *et al* 2014 that compared the expression profile of S. cerevisiae between mid-exponential growth phase with early stationary phase [27]. A 2-fold change threshold was used to identify differentially expressed genes. Lysine acetylation and protein phosphorylation data were obtained from the Weinert *et al* 2014 study that compared PTM levels between exponentially growing and stationary phase cells using *stable isotope labeling with amino acids in cell culture* (SILAC) [26]. A 2-fold change threshold of the protein-normalized PTM data was used to identify differentially expressed PTMs. Proteomics data was taken from Murphy *et al* time-course proteomics study [25]. The hoteling T2 statistic defined by the authors was used to identify proteins differentially expressed during diauxic shift; the top 25% of the differentially expressed proteins were assumed to be regulated. Proteomics data from Weinert *et al* was also used as an additional control and we observed the same trends using this data as well (S. Table 10). Further, we repeated the analysis after removing genes that were not expressed during transition to stationary phase; the transcripts for a total of 12 genes out of the 910 in the model were not detected by RNA-sequencing in the Treu *et al* study [27]. Removing the 12 genes did not impact any of the results (S. Table 9).

As additional validation, we used periodic data from the yeast cell cycle. Time-course SILAC phospho-proteomics data was obtained from Touati *et al* [37]. Phospho-sites whose abundance declined to less than 50% or increased by more than 50% at least two consecutive timepoints were considered dephosphorylated or phosphorylated respectively as defined by the authors. Transcriptomics data was taken from Kelliher *et al* study that identified 1246 periodic transcripts using periodicity-ranking algorithms [38].

The phospho-proteomics and transcriptome data during nitrogen shift was obtained from Oliveira *et al* [35,36]. The nitrogen shift studies compared the impact of adding glutamine to yeast cells growing on a poor nitrogen source (proline alone or glutamine depletion) with cells growing on a rich nitrogen source (glutamine plus proline). A 2-fold change threshold was used to identify differentially expressed transcripts and phospho-sites.

209 *E. coli* acetylation data was taken from the Weinert *et al* study comparing actively growing exponential
210 phase cells to stationary phase cells [42]. Proteomics and transcriptomics were from Houser *et al* study
211 of *E. coli* cells in early exponential phase and stationary phase [41]. Phospho-proteomics data for
212 exponential and early stationary phase *E. coli* cells was taken form Soares *et al* [40]. We used a 2-fold
213 change ($p < 0.05$) threshold for all studies.

214 The results are robust to the thresholds used for identifying differentially expressed genes or proteins
215 (S. Table 11). In all studies, genes and proteins that are either up or down regulated were considered to
216 be regulated. The final data set table used for all comparative analyses is provided as a supplementary
217 material (S. Table 13).

218

Genome scale metabolic modeling

220 We used the yeast metabolic network reconstruction (Yeast 7) by Aung *et al*, which contains 3,498
221 reactions, 910 genes and 2,220 metabolites [29]. The analysis of *E. coli* data was done using the
222 IJO1366 metabolic model [45]. All analyses were performed using COBRA toolbox for MATLAB [46].

223 The impact of gene knockouts on growth was determined using flux balance analysis (FBA). FBA
224 identifies an optimal flux through the metabolic network that maximizes an objective, usually the
225 production of biomass. A minimal glucose media (default condition) was used to determine the impact
226 of gene knockouts. Further, gene knockout analysis was repeated in a set of 87 different minimal
227 nutrient conditions to identify genes that impact growth across diverse conditions; these conditions
228 span all carbon and nitrogen sources that can support growth in the Yeast 7 model. The number of
229 times each gene was found to be lethal (growth < 0.01 units) across all conditions was used as a metric
230 of essentiality.

231 To infer topological properties, a reaction adjacency matrix was created by connecting reactions that
232 share metabolites. We used the Centrality toolbox function in MATLAB to infer all network topological
233 attributes including centrality, degree and PageRank.

234 Flux Variability Analysis (FVA) was used to infer the range of fluxes possible through every reaction in
235 the network. Two sets of flux ranges were obtained with FVA – the first with optimal biomass and the
236 latter without assuming optimality. In the second case, the fluxes are limited by the availability of
237 nutrients and energetics alone, thus it reflects the full range of metabolic activity possible in a cell.
238 Reactions with maximal flux above 900 units were assumed to be unconstrained and were excluded
239 from the analysis, as they are likely due to thermodynamically infeasible internal cycles [47]; the choice
240 of this threshold for flagging unconstrained reactions did not impact the distribution between regulators
241 over a wide range of values (S. Table 12).

242 For fitting experimentally derived flux data from Hackett *et al* [21], reactions were fit to the fluxes using
243 linear optimization and the flux through remaining reactions that do not have experimentally derived flux
244 data were inferred using FVA. Analysis using a related approach for inferring fluxes – PFBA, did not
245 reveal any significant difference as PFBA eliminates futile cycles and redundancy by minimizing total
246 flux through the network while maximizing for biomass [48] (S. Figure 5).

247 Reaction reversibility was determined directly from the model annotations. We also used additional
248 reversibility annotation from Martinez *et al* based on thermodynamics analysis of the Yeast metabolic
249 model [49]. Pathway annotations, enzyme molecular weight and catalytic activity values were obtained

250   from Sanchez *et al* [50]. The comparative analysis of regulatory mechanisms was also repeated using
251   the updated Yeast 7.6 model and yielded similar results (S. Table 8) [50].

252   The comparative analysis of target properties was done using gene-reaction pairs rather than genes or
253   reactions alone; the gene-reaction pairs accounts for regulation involving all possible combinations of
254   genes and associated reaction, including isozymes that may involve different genes but the same
255   reaction or multi-functional enzymes involving same the gene associated with different reactions. The
256   910 genes and 2310 gene-associated reactions resulted in 3375 unique gene-reaction pairs in yeast.

257   All statistical tests were performed using MATLAB. Significance of overlap between lists was estimated
258   using the hypergeometric test. Significance of the differences in distribution of target properties
259   between mechanisms were determined using ANOVA, the non-parametric Kruskal-Wallis test, and after
260   multiple hypothesis correction (S. Table 8).

Figures
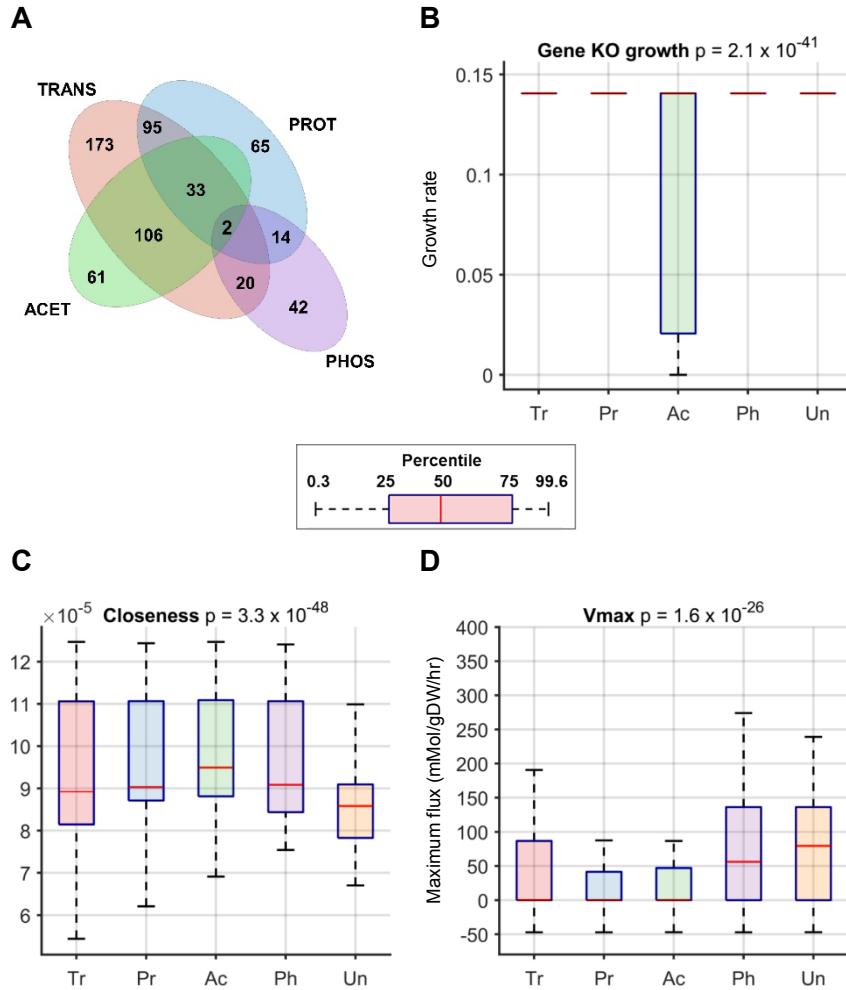
Figure 1. Comparison of the properties of the targets of regulation in yeast during transition to stationary phase. A. The Venn diagram shows the extent of overlap between targets of each process. Only 2 genes were found to be regulated by all four mechanisms. Targets of phosphorylation did not show any significant overlap with other mechanisms, while transcriptome and proteome showed the highest overlap (S. Table 1). **B.** Enzymes that impact growth when knocked out are highly likely to be acetylated. **C.** Enzymes with poor connectivity, as measured through the network connectivity metric - closeness, are more likely to be Unregulated. **D.** Enzymes catalyzing reactions with high maximum flux are likely to be either regulated through phosphorylation or to be unregulated. The Anova p-value comparing the differences in means is shown in the title. (Abbreviation: transcription (Tr), post-transcription (Pr), acetylation (Ac), phosphorylation (Ph) or Unregulated (Un)).

A
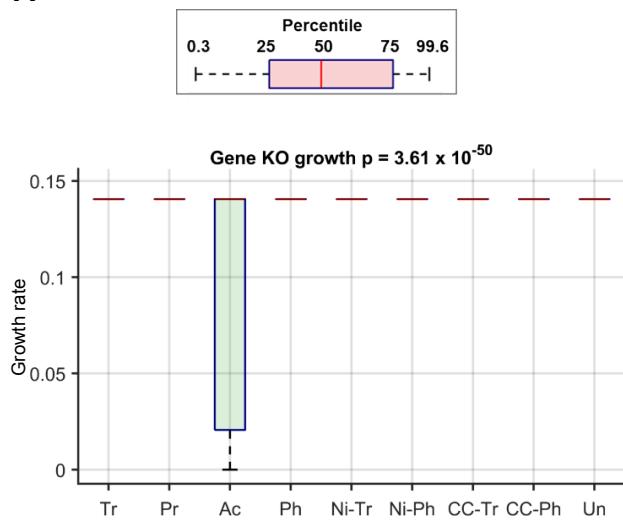
B
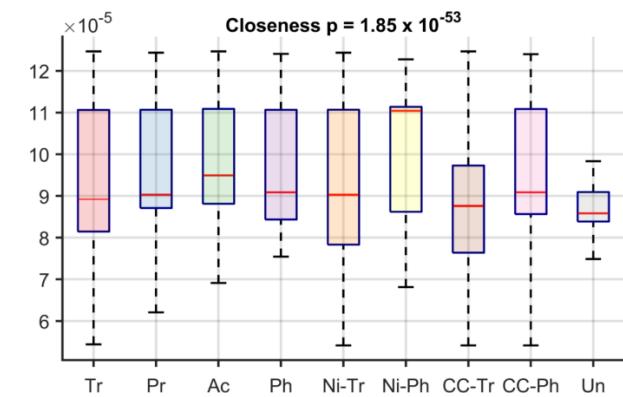
C
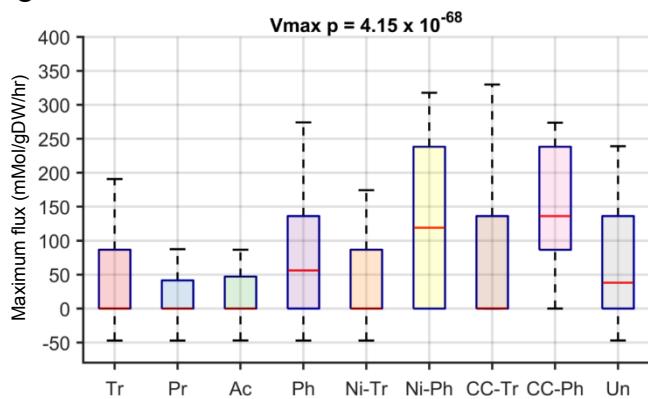
Figure 2. Comparison of the properties of enzymes in yeast regulated by each mechanism during the cell cycle (CC-Tr, CC-Ph) and nitrogen starvation (Ni-Tr, Ni-Ph). Data from stationary phase conditions (transcription (Tr), post-transcription (Pr), acetylation (Ac), phosphorylation (Ph) or Unregulated (Un)) are shown for comparison. Similar to stationary phase, enzymes that impact growth when knocked out are likely to be acetylated **(A),** enzymes that are highly connected are likely to be regulated by one of the four mechanisms **(B)** and those that catalyze reactions with high flux are likely to be regulated through phosphorylation in all three conditions **(C)**. The Anova p-value comparing the differences in means is shown in the title.
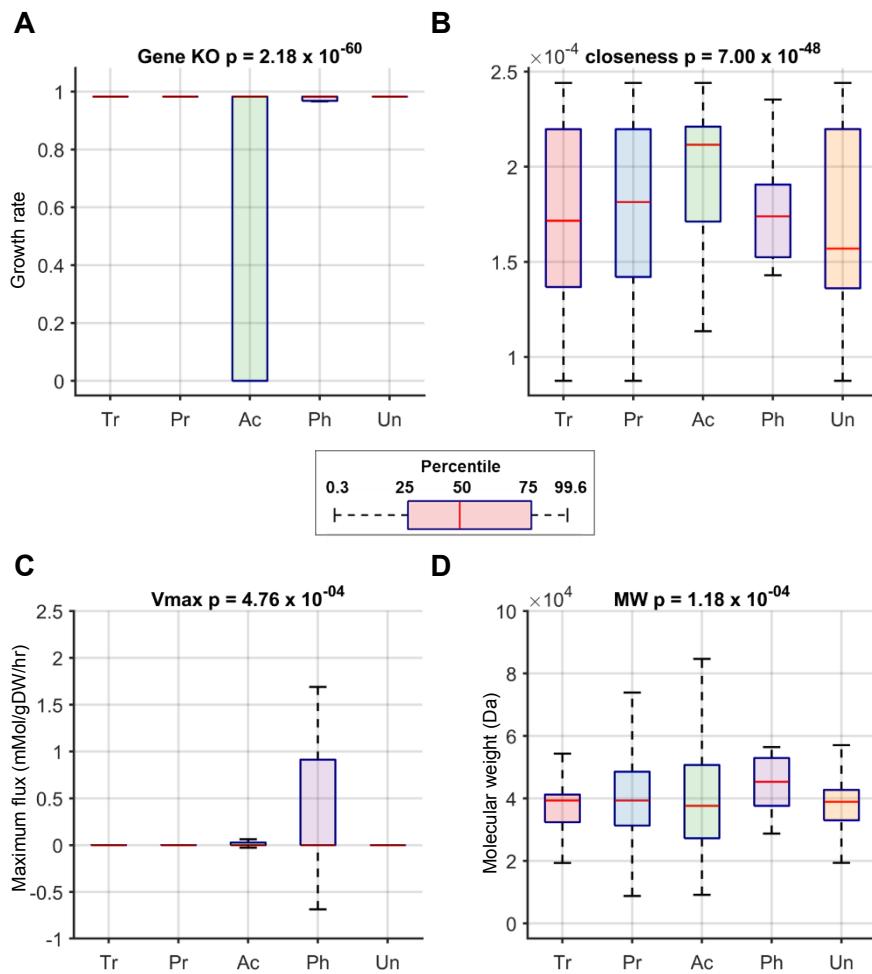
Figure 3. Comparison of the properties of enzymes in *E. coli* regulated by transcription (Tr), post-transcription (Pr), acetylation (Ac), phosphorylation (Ph) or Unregulated (Un) during transition to stationary phase. Similar to yeast, reaction essentiality **(A)**, connectivity **(B)**, maximum flux **(C)** and molecular weight (**D**) are predictive of regulation by acetylation, all four mechanisms, and phosphorylation (Vmax, MW) respectively.

A

	TRANS	PROT	ACET	PHOS
1. Essential	0.6443	-10.09	6.646	-0.343
2. High flux	-4.182	-2.85	-0.4459	7.242
3. High MW	-12.1	0.4925	-1.98	19.15
4. High closeness	2.647	6.621	4.758	7.558
5. Reversible	-14.72	-0.6941	-1.376	-3.028

Enrichment

20
10
0   log10(p-value)
-10
-20 Depletion

B

Biomass
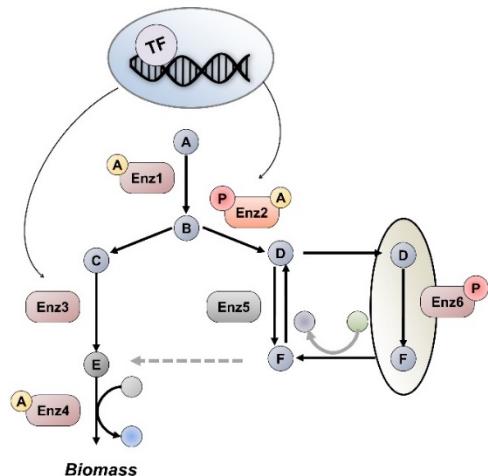
Figure 4. Reaction attributes predictive of regulation by each process in yeast. **A.** The heatmap shows the statistical enrichment and depletion of the targets of each process among reactions that are - (1) essential, (2) have high maximum flux (Vmax > 75th percentile), (3) catalyzed by enzymes with high molecular weight (MW > 75th percentile), (4) highly connected (Closeness > 75th percentile), and (5) reversible. The log-transformed p-values from hypergeometric test are shown with a positive sign for enrichment and negative sign for depletion. **B.** A schematic pathway summarizing the division of labor in metabolic regulation. Essential reactions (Enz1 and Enz4) are preferentially acetylated; reactions in futile cycles and in different compartments (Enz6) are phosphorylated; non-essential enzymes with low connectivity are regulated through transcriptional regulation (Enz3), and reactions with high connectivity are regulated through multiple mechanisms (Enz2). Reversible reactions are predominantly unregulated (Enz5).

261

266

267

References

1. Nielsen J. Systems Biology of Metabolism. Annu Rev Biochem. 2017; doi:10.1146/annurev-biochem-061516-044757

2. Cho BK, Zengler K, Qiu Y, Park YS, Knight EM, Barrett CL, et al. The transcription unit architecture of the Escherichia coli genome. Nat Biotechnol. 2009; doi:10.1038/nbt.1582

3. Chubukov V, Gerosa L, Kochanowski K, Sauer U. Coordination of microbial metabolism. Nature Reviews Microbiology. 2014. doi:10.1038/nrmicro3238

4. Heinemann M, Sauer U. Systems biology of microbial metabolism. Curr Opin Microbiol. 2010/03/12. 2010;13: 337–343. doi:10.1016/j.mib.2010.02.005

5. Aebersold R, Agar JN, Amster IJ, Baker MS, Bertozzi CR, Boja ES, et al. How many human proteoforms are there? Nature Chemical Biology. 2018. doi:10.1038/nchembio.2576

6. Kochanowski K, Sauer U, Noor E. Posttranslational regulation of microbial metabolism. Curr Opin Microbiol. 2015;27: 10–17.

7. Ihmels J, Levy R, Barkai N. Principles of transcriptional control in the metabolic network of Saccharomyces cerevisiae. Nat Biotechnol. 2004; doi:10.1038/nbt918

8. Stadtman ER. Mechanisms of Enzyme Regulation in Metabolism. Enzymes. 1970; doi:10.1016/S1874-6047(08)60171-7

9. Buescher JM, Liebermeister W, Jules M, Uhr M, Muntel J, Botella E, et al. Global network reorganization during dynamic adaptations of Bacillus subtilis metabolism. Science (80-). 2012; doi:10.1126/science.1206871

10. Daran-Lapujade P, Rossell S, van Gulik WM, Luttik MAH, de Groot MJL, Slijper M, et al. The fluxes through glycolytic enzymes in Saccharomyces cerevisiae are predominantly regulated at posttranscriptional levels. Proc Natl Acad Sci. 2007; doi:10.1073/pnas.0707476104

11. Holzer H, Duntze W. Metabolic Regulation by Chemical Modification of Enzymes. Annu Rev Biochem. 1971; doi:10.1146/annurev.bi.40.070171.002021

12. Fell D, Cornish-Bowden A. Understanding the control of metabolism. Portland press London; 1997.

13. Stadtman ER, Chock PB. Interconvertible Enzyme Cascades in Metabolic Regulation. Current Topics in Cellular Regulation. 1978. doi:10.1016/B978-0-12-152813-3.50007-0

14. Zhao S, Xu W, Jiang W, Yu W, Lin Y, Zhang T, et al. Regulation of cellular metabolism by protein lysine acetylation. Science (80-). 2010;327: 1000–1004.

298 15. Oliveira AP, Ludwig C, Picotti P, Kogadeeva M, Aebersold R, Sauer U. Regulation of yeast
299   central metabolism by enzyme phosphorylation. Mol Syst Biol. 2012; doi:10.1038/msb.2012.55

300 16. Zaslaver A, Mayo AE, Rosenberg R, Bashkin P, Sberro H, Tsalyuk M, et al. Just-in-time
301   transcription program in metabolic pathways. Nat Genet. 2004; doi:10.1038/ng1348

302 17. Lee JM, Gianchandani EP, Eddy JA, Papin JA. Dynamic analysis of integrated signaling,
303   metabolic, and regulatory networks. PLoS Comput Biol. 2008/05/17. 2008;4: e1000086.
304   doi:10.1371/journal.pcbi.1000086

305 18. Covert MW, Knight EM, Reed JL, Herrgard MJ, Palsson BO. Integrating high-throughput and
306   computational data elucidates bacterial networks. Nature. 2004/05/07. 2004;429: 92–96.
307   doi:10.1038/nature02456nature02456 [pii]

308 19. Shen F, Boccuto L, Pauly R, Srikanth S, Chandrasekaran S. Genome-scale network model of
309   metabolism and histone acetylation reveals metabolic dependencies of histone deacetylase
310   inhibitors. Genome Biol. 2019;20: 49. doi:10.1186/s13059-019-1661-z

311 20. Chandrasekaran S, Price ND. Probabilistic integrative modeling of genome-scale metabolic and
312   regulatory networks in Escherichia coli and Mycobacterium tuberculosis. Proc Natl Acad Sci.
313   National Acad Sciences; 2010;107: 17845–17850.

314 21. Hackett SR, Zanotelli VRT, Xu W, Goya J, Park JO, Perlman DH, et al. Systems-level analysis of
315   mechanisms regulating yeast metabolic flux. Science (80-). 2016; doi:10.1126/science.aaf2786

316 22. Almaas E, Kovács B, Vicsek T, Oltvai ZN, Barabási AL. Global organization of metabolic fluxes
317   in the bacterium Escherichia coli. Nature. 2004; doi:10.1038/nature02289

318 23. Stelling J, Klamt S, Bettenbrock K, Schuster S, Gilles ED. Metabolic network structure
319   determines key aspects of functionality and regulation. Nature. 2002; doi:10.1038/nature01166

320 24. Stelling J, Sauer U, Szallasi Z, Doyle FJ, Doyle J. Robustness of cellular functions. Cell. 2004.
321   doi:10.1016/j.cell.2004.09.008

322 25. Murphy JP, Stepanova E, Everley RA, Paulo JA, Gygi SP. Comprehensive Temporal Protein
323   Dynamics during the Diauxic Shift in Saccharomyces cerevisiae . Mol Cell Proteomics. 2015;
324   doi:10.1074/mcp.m114.045849

325 26. Weinert BT, Iesmantavicius V, Moustafa T, Schölz C, Wagner SA, Magnes C, et al. Acetylation
326   dynamics and stoichiometry in Saccharomyces cerevisiae. Mol Syst Biol. 2014;10: 716.

327 27. Treu L, Campanaro S, Nadai C, Toniolo C, Nardi T, Giacomini A, et al. Oxidative stress response
328   and nitrogen utilization are strongly variable in Saccharomyces cerevisiae wine strains with
329   different fermentation performances. Appl Microbiol Biotechnol. 2014; doi:10.1007/s00253-014-
330   5679-6

331 28. Beltrao P, Bork P, Krogan NJ, Van Noort V. Evolution and functional cross-talk of protein post-
332   translational modifications. Molecular Systems Biology. 2013. doi:10.1002/msb.201304521

333 29. Aung HW, Henry SA, Walker LP. Revising the representation of fatty acid, glycerolipid, and
334   glycerophospholipid metabolism in the consensus model of yeast metabolism. Ind Biotechnol.
335   2013;9: 215–228. doi:10.1089/ind.2013.0013

336 30. Oliveira AP, Sauer U. The importance of post-translational modifications in regulating
337   Saccharomyces cerevisiae metabolism. FEMS Yeast Research. 2012. doi:10.1111/j.1567-
338   1364.2011.00765.x

339 31. Beltrao P, Albanèse V, Kenner LR, Swaney DL, Burlingame A, Villén J, et al. Systematic
340   functional prioritization of protein posttranslational modifications. Cell. 2012;
341   doi:10.1016/j.cell.2012.05.036

342 32. Orth JD, Thiele I, Palsson BØ. What is flux balance analysis? Nat Biotechnol. Nature Research;
343   2010;28: 245–248. doi:10.1038/nbt.1614

344 33. Schuetz R, Zamboni N, Zampieri M, Heinemann M, Sauer U. Multidimensional optimality of
345   microbial metabolism. Science (80-). 2012; doi:10.1126/science.1216882

346 34. Mahadevan R, Schilling CH. The effects of alternate optimal solutions in constraint-based
347   genome-scale metabolic models. Metab Eng. 2003;5: 264–276.
348   doi:10.1016/j.ymben.2003.09.002

349 35. Oliveira AP, Dimopoulos S, Busetto AG, Christen S, Dechant R, Falter L, et al. Inferring causal
350   metabolic signals that regulate the dynamic TORC1-dependent transcriptome. Mol Syst Biol.
351   2015; doi:10.15252/msb.20145475

352 36. Oliveira AP, Ludwig C, Zampieri M, Weisser H, Aebersold R, Sauer U. Dynamic
353   phosphoproteomics reveals TORC1-dependent regulation of yeast nucleotide and amino acid
354   biosynthesis. Sci Signal. 2015; doi:10.1126/scisignal.2005768

355 37. Touati SA, Kataria M, Jones AW, Snijders AP, Uhlmann F. Phosphoproteome dynamics during
356   mitotic exit in budding yeast. EMBO J. 2018; doi:10.15252/embj.201798745

357 38. Kelliher CM, Leman AR, Sierra CS, Haase SB. Investigating Conservation of the Cell-Cycle-
358   Regulated Transcriptional Program in the Fungal Pathogen, Cryptococcus neoformans. PLoS
359   Genet. 2016; doi:10.1371/journal.pgen.1006453

360 39. Amoutzias GD, He Y, Gordon J, Mossialos D, Oliver SG, Van de Peer Y. Posttranslational
361   regulation impacts the fate of duplicated genes. Proc Natl Acad Sci. 2010;
362   doi:10.1073/pnas.0911603107

363 40. Soares NC, Spät P, Krug K, MacEk B. Global dynamics of the Escherichia coli proteome and
364   phosphoproteome during growth in minimal medium. J Proteome Res. 2013;
365   doi:10.1021/pr3011843

366 41. Houser JR, Barnhart C, Boutz DR, Carroll SM, Dasgupta A, Michener JK, et al. Controlled
367   Measurement and Comparative Analysis of Cellular Components in E. coli Reveals Broad
368   Regulatory Changes in Response to Glucose Starvation. PLoS Comput Biol. 2015;
369   doi:10.1371/journal.pcbi.1004400

370 42. Weinert BT, Iesmantavicius V, Wagner SA, Schölz C, Gummesson B, Beli P, et al. Acetyl-
371   phosphate is a critical determinant of lysine acetylation in E. coli. Mol Cell. 2013;51: 265–272.

372 43. Humphrey SJ, James DE, Mann M. Protein Phosphorylation: A Major Switch Mechanism for
373   Metabolic Regulation. Trends in Endocrinology and Metabolism. 2015.
374   doi:10.1016/j.tem.2015.09.013

375 44. Choi KR, Jang WD, Yang D, Cho JS, Park D, Lee SY. Systems Metabolic Engineering
376   Strategies: Integrating Systems and Synthetic Biology with Metabolic Engineering. Trends in
377   Biotechnology. 2019. doi:10.1016/j.tibtech.2019.01.003

378 45. Orth JD, Conrad TM, Na J, Lerman JA, Nam H, Feist AM, et al. A comprehensive genome-scale
379   reconstruction of Escherichia coli metabolism--2011. Mol Syst Biol. 2011/10/13. 2011;7: 535.
380   doi:10.1038/msb.2011.65

381 46. Becker SA, Feist AM, Mo ML, Hannum G, Palsson BO, Herrgard MJ. Quantitative prediction of
382   cellular metabolism with constraint-based models: the COBRA Toolbox. Nat Protoc. 2007/04/05.
383   2007;2: 727–738. doi:nprot.2007.99 [pii]10.1038/nprot.2007.99

384 47. Schellenberger J, Lewis NE, Palsson B. Elimination of thermodynamically infeasible loops in
385   steady-state metabolic models. Biophys J. 2011; doi:10.1016/j.bpj.2010.12.3707

386 48. Lewis NE, Hixson KK, Conrad TM, Lerman JA, Charusanti P, Polpitiya AD, et al. Omic data from
387   evolved E. coli are consistent with computed optimal growth from genome-scale models. Mol
388   Syst Biol. 2010;6: 390.

389 49. Martínez VS, Quek LE, Nielsen LK. Network thermodynamic curation of human and yeast
390   genome-scale metabolic models. Biophys J. 2014; doi:10.1016/j.bpj.2014.05.029

391 50. Sánchez BJ, Zhang C, Nilsson A, Lahtvee P, Kerkhoven EJ, Nielsen J. Improving the phenotype
392   predictions of a yeast genome-scale metabolic model by incorporating enzymatic constraints.
393   Mol Syst Biol. 2017; doi:10.15252/msb.20167411

394

395

396

397

398

399

400

401

402

403

404

405

406

407

408

409

410

411

412

413

414 **Supplementary Figures**

415

416

417

growth across conditions $p = 7.16 \times 10^{-41}$
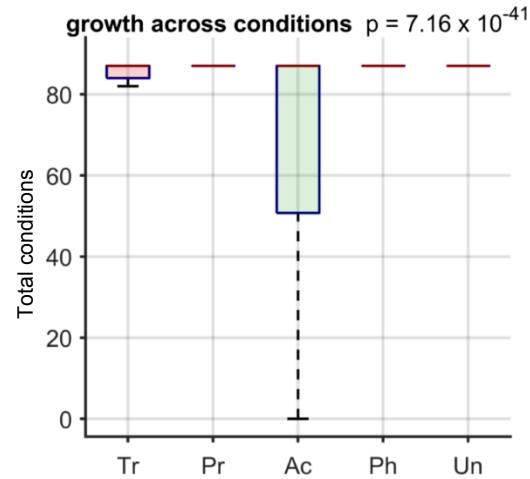
418

419

420 **S. Figure 1.** Distribution of regulation based on gene essentiality across 87 different conditions. These
421 conditions comprise 56 different carbon sources including glucose, and 31 different nitrogen sources
422 including ammonium ions. The total number of conditions in which each gene deletion was viable was
423 calculated. This total number was then compared between targets of each regulatory mechanism. The
424 box plots show that acetylation preferentially regulates the genes that impact growth across the 87
425 conditions. The box plot whiskers extend to the 99.3rd percentile of each distribution. The ANOVA p-
426 value comparing the means is 7.1×10^{-41}.

427

428

429

430

431

432

433

434

435

436

437

S. Figure 2. Distribution of regulation based on topological properties of each reaction. Four different topological properties are shown in the box plots - the total number of annotated pathways each reaction participates (Tot. pathways), the number of times each reaction is traversed during a random walk between reactions in the network (Pagerank), the total number of connected reactions (Degree) and the number of times each reaction appears on a shortest path between two reactions (Betweenness). These show that reactions that are regulated by any mechanism have a higher connectivity compared to those that are unregulated. Furthermore, reactions regulated by both acetylation and phosphorylation had the highest connectivity across all metrics. The ANOVA p-value comparing the means is provided in the title. (Abbreviations: regulation by both transcription and post-transcription (Tr + Pr), both acetylation and phosphorylation (Ac + Ph), at least 3 regulators (3 Reg), and Unregulated (Un)).

17

S. Figure 3. Properties of reactions regulated by multiple mechanisms. The box plots compare the properties of enzymes regulated by transcription, post-transcription, acetylation, phosphorylation with those regulated by both transcription and post-transcription (Tr + Pr), both acetylation and phosphorylation (Ac + Ph), or at least 3 regulators (3 Reg). This set of combinations among regulators was chosen as both acetylation and phosphorylation are PTMs, and the transcriptome and proteome of yeast cells show significant correlation. Reactions regulated by both acetylation and phosphorylation had the highest connectivity as measured by the inverse sum of the distance from a reaction to all other reactions in the network (Closeness). Apart from connectivity, reactions regulated by two different mechanisms did not share properties of reactions regulated by each individual mechanism. For example, reactions regulated by acetylation and phosphorylation were not likely to be essential or have high maximum flux. The ANOVA p-value comparing the means is provided in the title.

470

471 **S. Figure 4.** The box plots show the distribution of regulation based on reaction reversibility. Reversible
472 reactions were highly likely to be not regulated by any of the four mechanisms. The left panel compares
473 the distribution of regulation of reversible reactions based on the annotation from the Yeast 7 model
474 (reversible reactions are set to 1 and irreversible reactions are set to 0). The panel on the right uses an
475 updated list based on thermodynamic analysis of the Yeast metabolic model by Martinez *et al* [49].

476

477

478

479

480

481

482

483

484

485

486

487

488

489

490

491

S. Figure 5. Distribution of regulation based on magnitude of maximum possible flux (mmol/gDW/hr) through each reaction. The plots compare the distribution of regulation using flux calculated using various methods and models. The ANOVA p-value comparing the means is provided in the panel title of each plot. These results show that phosphorylated reactions are highly enriched among those reactions with high maximum flux. **A.** Maximum flux through each reaction was calculated using FVA using the Yeast 7 model without assuming that cells maximize their biomass (the default objective in FVA and FBA). The box plots compare the maximum flux value of reactions regulated by each mechanism. **B.** Maximum flux through each reaction was calculated using FVA without assuming that cells maximize their biomass using the Yeast 7.6 model (Yeast 7 model was used for all analyses). **C.** The flux through

20

501   the model was first fit to the experimentally inferred flux data from Hackett *et al*[21]. The maximum flux
502   through all reactions was then determined using FVA. **D.** The flux through each reaction was inferred
503   from Parsimonious FBA (PFBA). Note that PFBA does not provide the maximum flux but the flux value
504   that minimizes the sum of flux through all reactions while maximizing the biomass objective. Hence it
505   does not reveal any futile cycles or redundancy in the network. **E.** The heatmap shows the distribution
506   of regulation based on magnitude of maximum possible flux (Vmax) through of each reaction.
507   Reactions are sorted based on Vmax inferred from FVA. The columns correspond to each reaction-
508   gene pair. Those that are regulated by each mechanism are shown in yellow, while those that are not
509   regulated by a specific mechanism are in blue.

510

511
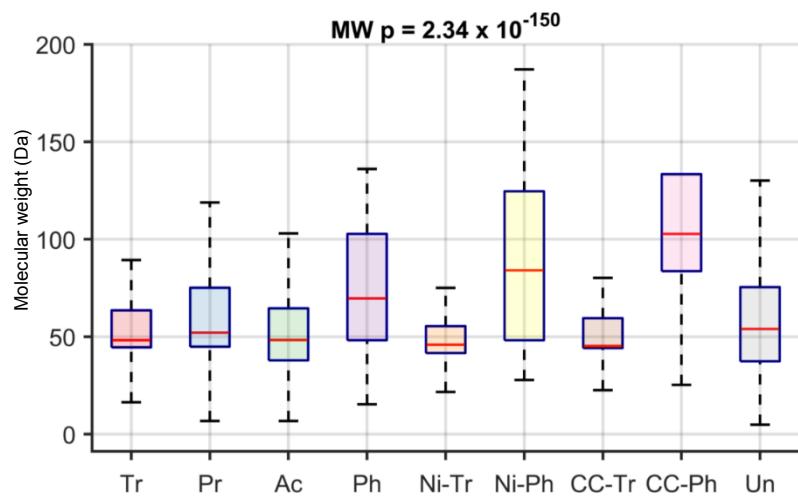
513   **S. Figure 6.** The box plots show the distribution of regulation in Yeast based on enzyme molecular
514   weight. Enzymes regulated by phosphorylation on average tended to have high molecular weight. Data
515   for targets of phosphorylation and transcriptional regulation in Nitrogen starvation (denoted by 'Ni_'
516   prefix) and Cell cycle (denoted by 'CC_' prefix) conditions are also shown for comparison.

517

518

519

520

521

S. Figure 7. The box plots show the distribution of regulation based on enzyme catalytic activity (kcat) in Yeast (data from Sanchez *et al* [50]). No consistent difference across datasets was observed in regulation based on the catalytic activity of the target enzyme.

525

526

527

528

529

530

531

532

533

534

535

536

537

538

539

540

541

542

543

22
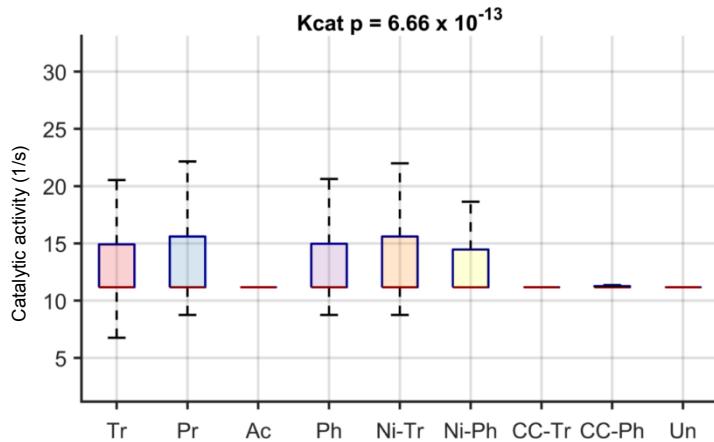
544

545 **Supplementary Tables**

546 **A**

Regulatory mechanisms		Reaction Overlap	p-value
TRANS	PROT	421	4.12×10^{-30}
TRANS	ACET	285	2.36×10^{-19}
TRANS	PHOS	266	0.241723
PROT	ACET	133	8.53×10^{-05}
PROT	PHOS	117	0.925481
ACET	PHOS	89	0.420549

547

548 **B**

Regulatory mechanisms		Gene Overlap	p-value
TRANS	PROT	153	0.010941
TRANS	ACET	157	0.001552
TRANS	PHOS	61	0.931005
PROT	ACET	69	0.925509
PROT	PHOS	42	0.291789
ACET	PHOS	34	0.860463

549

550 **C**

Total regulators	Percentage among those regulated
2 or more	47.8%
3 or more	8.7%
All 4	0.08%

551

552 **S. Table 1.** Overlap between targets of various mechanisms - transcription (TRANS), post-transcription
553 (PROT), acetylation (ACET), phosphorylation (PHOS). This reveals low overlap between targets of
554 regulation by phosphorylation and other mechanisms. **A.** Overlap between target reactions **B.** Overlap
555 between target genes. **C.** Percentage of reactions regulated by multiple mechanisms. Overall, 69% of
556 the gene-associated reactions in the model were regulated; among those regulated, 47.8% were
557 regulated by more than one mechanism.

558

559 **S. Table 2.** Essential reactions regulated by acetylation (Spreadsheet file)

560

561 **S. Table 3.** Top 50 reactions sorted based on topological connectivity (Spreadsheet file)

562

563 **S. Table 4.** Top 50 reactions with maximum reaction flux regulated by phosphorylation (Spreadsheet
564 file)

23

565

Regulation	*E. coli*	S. cerevisiae
Transcription	469	468
Post-transcription/Proteomic	372	266
Acetylation	460	265
Phosphorylation	17	133

566

567 **S. Table 5.** Comparison of total genes regulated by each process in *E. coli* with *S. cerevisiae* shows
568 that phosphorylation plays a relatively minor role in *E. coli* metabolic regulation during stationary phase.

569

570

Regulatory mechanisms		p-value	Reaction Overlap
TRANS	PROT	3.77×10^{-23}	590
ACET	TRANS	0.042022	442
ACET	PROT	0.192068	379
ACET	PHOS	5.60×10^{-11}	28
PHOS	TRANS	0.004853	22
PHOS	PROT	0.95148	9

571

572 **S. Table 6.** Overlap between targets of various mechanisms in *E. coli* - transcription (TRANS), post-
573 transcription (PROT), acetylation (ACET), phosphorylation (PHOS).

574

575

576 **S. Table 7.** Gaps in regulation – Essential genes that are unregulated. One representative reaction is
577 shown for each gene in case there are multiple reactions associated with it (Spreadsheet file)

578

579

Model	Yeast 7 (default)		Yeast 7.6	
p-value	ANOVA	Kruskal-Wallis	ANOVA	Kruskal-Wallis
Growth rate	2.07×10^{-41}	1.24×10^{-29}	7.82×10^{-43}	1.37×10^{-47}
Closeness	3.33×10^{-48}	1.74×10^{-55}	1.66×10^{-39}	3.61×10^{-51}
Vmax (without max. biomass)	5.53×10^{-26}	9.25×10^{-13}	6.97×10^{-8}	1.30×10^{-11}

580

581 **S. Table 8.** Robustness of the results comparing the difference in distribution of properties between
582 targets of various regulatory mechanisms using the Yeast 7.6 model. Significance of results using the
583 non-parametric Kruskal-Wallis test is also shown. The p-values for the key reaction features shown in
584 Figure 1 using the Yeast 7 model is provided as comparison. All p-values are significant at FDR < 0.01
585 using both Bonferroni adjustment and Benjamin-Hochberg multiple hypothesis correction.

586

587

Model	All genes (default)		All expressed genes	
p-value	ANOVA	Kruskal-Wallis	ANOVA	Kruskal-Wallis
Growth rate	2.07×10^{-41}	1.24×10^{-29}	3.3×10^{-41}	2.1×10^{-29}
Closeness	3.33×10^{-48}	1.74×10^{-55}	2.2×10^{-49}	3.5×10^{-56}
Vmax	1.59×10^{-26}	2.51×10^{-21}	8.1×10^{-27}	1.3×10^{-21}

588

589 **S. Table 9.** Robustness of the results after removing genes that are not-expressed (i.e. not detected in
590 RNA-seq data) in both exponential and stationary phase cultures. The p-values reported in Figure 1
591 using all the metabolic genes in the Yeast 7 model is provided as comparison.

592

593

594

Model	Murphy *et al* (default)		Weinert *et al*	
p-value	ANOVA	Kruskal-Wallis	ANOVA	Kruskal-Wallis
Growth rate	2.07×10^{-41}	1.24×10^{-29}	1.59×10^{-37}	2.63×10^{-33}
Closeness	3.33×10^{-48}	1.74×10^{-55}	3.10×10^{-44}	1.62×10^{-48}
Vmax	1.59×10^{-26}	2.51×10^{-21}	1.71×10^{-22}	1.94×10^{-19}

595

596 **S. Table 10.** Comparison of results using proteomics data from Weinert *et al* instead of Murphy *et al*.
597 The ANOVA p-value comparing the means are provided. The p-values reported in Figure 1 using
598 Murphy *et al* data is provided as comparison.

599

600

601

Fold change	2 (default)	1.5	3	4
Growth rate	2.07×10^{-41}	3.72×10^{-35}	1.12×10^{-34}	5.82×10^{-26}
Closeness	3.33×10^{-48}	2.09×10^{-47}	1.13×10^{-32}	6.95×10^{-20}
Vmax (with max. biomass)	1.59×10^{-26}	6.97×10^{-24}	1.26×10^{-23}	1.01×10^{-19}

602

Top Percentile	25 (default)	50	15	5
Growth rate	2.07×10^{-41}	1.42×10^{-42}	2.49×10^{-39}	2.71×10^{-40}
Closeness	3.33×10^{-48}	1.86×10^{-41}	7.15×10^{-55}	9.66×10^{-48}
Vmax (with max. biomass)	1.59×10^{-26}	6.07×10^{-18}	5.66×10^{-31}	8.98×10^{-36}

603

604 **S. Table 11.** Comparison of thresholds used for identifying differentially expressed genes and proteins.
605 These show that our results are robust to the thresholds for identifying the targets of various regulatory
606 mechanisms. The ANOVA p-value comparing the means are provided. Note that the first table uses
607 fold change thresholds for transcriptomics, acetylation and phospho-proteomics data alone. Since the

608 proteomics data uses a percentile cut off, the robustness analysis for this data was performed
609 separately.

610

611

Threshold for unconstrained reactions	ANOVA p-value for Vmax
100	5.07×10^{-31}
200	1.08×10^{-57}
300	5.27×10^{-50}
400	3.53×10^{-27}
500	2.24×10^{-25}
600	2.24×10^{-25}
700	2.24×10^{-25}
800	1.59×10^{-26}
900	1.59×10^{-26}
1000	4.68×10^{-150}

612

613 **S. Table 12.** Comparison of thresholds used for identifying unconstrained reactions from FVA.
614 Reactions with maximal flux above the threshold listed in the table were assumed to be unconstrained
615 and were excluded from the analysis, as they are likely due to thermodynamically infeasible internal
616 cycles. The ANOVA p-value comparing the means of the maximum flux through the target reactions of
617 different regulatory mechanisms is provided. The default value (900 mmol/gDW/hr) for eliminating
618 unconstrained reactions is highlighted and was used for all analyses. These show that our results are
619 robust to the thresholds for identifying unconstrained reactions.

620

621 **S. Table 13.** Raw dataset containing all yeast genes and associated reactions, the corresponding
622 regulators, and the reaction properties (Spreadsheet file).

623